ELSEVIER
CrossMark
Available online at www.sciencedirect.com
ScienceDirect
Procedia Engineering 120 (2015) 112 – 115
Procedia Engineering
www.elsevier.com/locate/procedia

EUROSENSORS 2015

Geometry study of an isotropic 3D Silicon Hall sensor

C. Sander*, C. Leube, T. Aftab, P. Ruther and O. Paul

Microsystem Materials Laboratory (MML), Department of Microsystems Engineering (IMTEK), University of Freiburg, Germany

Abstract

This paper reports a geometry study to evaluate the influence of design parameters on the performance of a novel three-dimensional (3D) Hall sensor. The focus is in particular on the isotropy of the sensitivities for the three spatial components of the magnetic field and the inherent offset voltage. The silicon Hall device has the shape of a hexagonal prism with symmetric sets of three contacts located on its top and bottom surfaces. By sending currents obliquely across the sensitive volume one is able to operate the device as three identical and mutually orthogonal Hall sensors. We demonstrate a design with isotropic sensitivities of about 34.3 mV/VT and an inherent offset of 2 mV which can be further reduced by an appropriate sensor redesign.

Peer-review under responsibility of the organizing committee of EUROSENSORS 2015

Keywords: Hall sensor; 3D Hall device; Triaxial sensor; Angular sensor

1. Introduction

Magnetic field transducers based on the Hall effect in silicon (Si) are used for applications in automobiles, industrial control systems, and consumer devices [1]. Traditional planar Hall effect transducers are sensitive to only one component of the magnetic flux density ***B***. For the purpose of measuring all three spatial components of ***B***, three separate, orthogonally aligned devices have been used. This cost-ineffective configuration is difficult to implement and unable to measure all ***B*** components at the same location [1]. An alternative approach is to co-integrate a planar Hall plate with two vertical Hall sensors (VHS) [2]. However, the vertical Hall structures show lower sensitivity and higher offsets and thus require separate signal conditioning circuitry for compensation [3]. Recently we presented the first 3D Hall device fabricated in Si technology providing the detection of all three orthogonal components of ***B*** with almost identical sensitivities and comparable offsets [4].

In this paper we address again this novel sensor concept and focus on a geometry study to evaluate the electrical response in terms of sensitivity and offset depending on the device geometry. Experimental results are compared to finite element (FE) simulation.

* Corresponding author. Tel.: +49-761-203-7193; fax: +49-761-203-7192.
E-mail address: christian.sander@imtek.de

1877-7058
Peer-review under responsibility of the organizing committee of EUROSENSORS 2015
doi:10.1016/j.proeng.2015.08.577

2. Sensor Concept

The ideal planar Hall effect device is a plate with four peripheral contacts and the symmetry of a square. Its output voltage can be written as $V_{\text{out}}(B) = V_{\text{H}}(B) + V_{\text{off}} = SV_{\text{in}}B + V_{\text{off}}$, where B, $S = V_{\text{in}}^{-1}dV_{\text{out}}/dB$, V_{H}, V_{in}, and $V_{\text{off}} = V_{\text{out}}(B = 0)$ denote the out-of-plane magnetic flux density, the voltage-related sensitivity, the Hall voltage, the drive voltage and the offset of the device in the absence of a magnetic field, respectively. Usually, V_{H} is obtained by the spinning-current method, where the driving and sensing contacts are cyclically permuted four times and the output voltages are averaged to effectively suppress V_{off}.

The construction of the novel device by deductive reasoning has been described previously [4]. The result is a structure with six contacts arranged as two groups of three contacts on each side of a semiconductor wafer, as shown in a perpendicular view in Fig. 1(a) and in perspective in Fig. 1(b). To enhance the magnetic sensitivity of the device, the current flow is contained in a hexagonally prismatic volume, cf. Fig. 1(b). The resulting structure is invariant under rotation by 120° around a perpendicular axis and it is centrosymmetric. As indicated in Fig. 1(b), it can be operated in three planes using three groups of four contacts. The sensitivity vectors $\boldsymbol{S}_i = (S_{ix}, S_{iy}, S_{iz})$ corresponding to these three planes are labeled by $i = 1, 2, 3$, where S_{ij} with $j = x, y, z$ is defined as $S_{ij} = (\partial V_{\text{H},i}/\partial B_j)/V_{\text{in}}$ where B_x, B_y, and B_z denote the three components $\boldsymbol{B}$ at the location of the sensor. They can be made orthogonal by appropriately dimensioning the device. In view of the 120° rotational symmetry of the device they have the same magnitude S_0. Figure 1(c) shows a micrograph of a sensor fabricated using double-sided insulation of a 5 Ωcm n-doped Si wafer, contact diffusion, metallization, and deep reactive ion etching [4]. As a result of the design, the hexagonal prism is suspended in a Si frame chip by six bridges with a height and width of about 255 µm and 100 µm, respectively. A schematic including the relevant geometry parameters, i.e., the hexagon side length a, the device thickness t, the contact length l and width w, respectively, is shown in Fig. 1(d). The geometry of this sensor design is completely captured by three independent design parameter ratios which are the relative device diameter $r_{\text{d}} = 2a/t$, the relative contact length $r_{\text{l}} = l/a$ and the relative contact width $r_{\text{w}} = w/a$. In this study the influence of the ratios r_{d} and r_{l} on the electrical response of the novel device is characterized. For this purpose five different sensors with design parameters listed in Table 1 were fabricated and mounted on a printed circuit board (PCB) carrier. For all devices $t = 525$ µm and $r_{\text{w}} = 0.019$ are fixed. The rear electrical interconnection of the devices to the carrier is performed by flip-chip bonding, whereas the front contacts are wire-bonded to it. An assembled device is shown in Fig. 1(e).

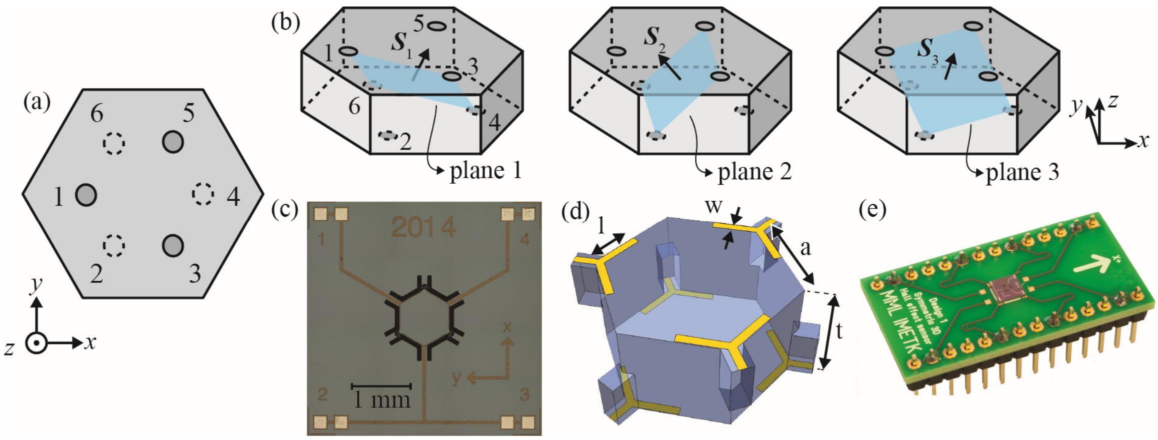

Figure 1: Schematic projection (a) of the novel 3D Hall sensor onto two parallel xy-planes, (b) perspective view of the hexagonal 3D Hall device with its three operation planes and respective sensitivity vectors $\boldsymbol{S}_1$, $\boldsymbol{S}_2$ and $\boldsymbol{S}_3$, (c) micrograph of the novel sensor, (d) schematic with relevant geometry parameters and (e) assembled device.

Table 1. Design parameters of the fabricated 3D Hall sensors.

design parameter	reference	#2	#3	#4	#5
r_d	**1.875**	1.8	1.95	1.875	1.875
r_l	**0.9**	0.9	0.9	0.85	0.95

3. Experimental Results

The devices were characterized using the parameter analyzer 4156C from Agilent. A 3D Helmholtz coil setup served to extract the electric field dependent sensitivities of the sensors up to 4 mT. As an example, the offset characteristic for one plane for the reference device is shown in Fig. 2. The measurement is performed in four modes applying the spinning-current method. The single-mode offset increases linearly with the input voltage V_{in}. The residual offset V_{res} obtained by averaging the four modes is reduced from about 11 mV to 16 µV at $V_{in} = 1$ V. The Hall voltage V_H of the reference device for all three operating planes is shown in Fig. 3. For each plane, three sensitivity values corresponding to B_x, B_y, and B_z are extracted forming the sensitivity vectors $\boldsymbol{S}_1$ to $\boldsymbol{S}_3$.

The figures of merit extracted from the measurements include the average input resistance $R_{in,av}$, the average absolute single mode offsets $V_{off,av}$ over all 12 modes using the sign of the first mode, the average voltage related sensitivity magnitude $S_0 = 1/3(S_1 + S_2 + S_3)$ and the average polar angle $\theta_{av} = (\theta_1 + \theta_2 + \theta_3)/3$ where θ_i is defined as the angle between the sensitivity vector $\boldsymbol{S}_i$ and the z axis. By the symmetry of the device $\boldsymbol{S}_1$ to $\boldsymbol{S}_3$ ideally have the same magnitude and can be transferred into each other by 120° rotations. Therefore the polar angles θ_1 to θ_3 are ideally equal. If $\theta_i = 54.7°$, $\boldsymbol{S}_1$ to $\boldsymbol{S}_3$ are orthogonal and the device is an isotropic magnetic field sensor.

The numerical and measured results in Figs. 4(a) and (b) focus on the variation of the device diameter ratio r_d, whereas Figs. 4(c) and (d) illustrate the results for a variable contact length ratio r_l. Further the data are listed in Table 2. In Fig. 4(a) $R_{in,av}$ decreases with increasing r_d. Further $V_{off,av}$ decreases by approximately 10 mV from 17 mV to 3 mV in the considered range. A qualitatively similar behavior is observed for the simulation. A device with zero offset seems to be feasible by further increasing r_d. The sensitivity magnitude S_0 is not affected by r_d, cf. Fig. 4(b), since scaling the device geometry in the xy plane leaves the size of the electrical contacts relative to the hexagon side length constant. For both measurement and simulation a decrease of θ_{av} with increasing r_d is shown in Fig. 4(b). The expansion of the device in the xy plane increases the in-plane current density which is responsible for the out-of-plane sensitivity component B_z. Consequently all three sensitivity vectors tend to the z axis resulting in a reduction of the polar angles θ_i and thus of θ_{av}. The results indicate that the ideal angle of $\theta_i = 54.7°$ can be achieved by further increasing r_d. By extrapolating the data to $r_d = 2$ an isotropic device with zero offset and a sensitivity of 34.6 mV/VT is obtained.

Figure 4(c) shows that R_{in} decreases with increasing r_l, due to the expansion of the contact regions. The variation of r_l has a non-linear influence on V_{off} as shown in Fig. 4(c). Measurement and simulation show an overall increase of approximately 30 mV in the

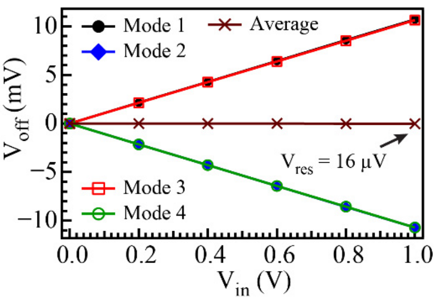

Figure 2: Offset voltage V_{off} and residual offset V_{res} after current spinning for the reference device.

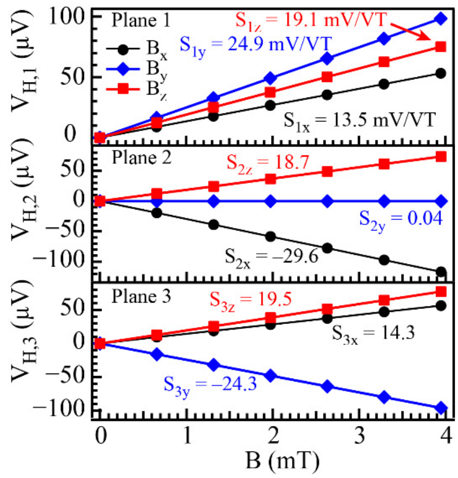

Figure 3: Hall voltage $V_{H,i}$ for each plane (i = 1,2,3) as a function of the spatial components of B_j ($j = x,y,z$) including the extracted sensitivities $S_{ij} = (\partial V_{H,i}/\partial B_j)/V_{in}$.

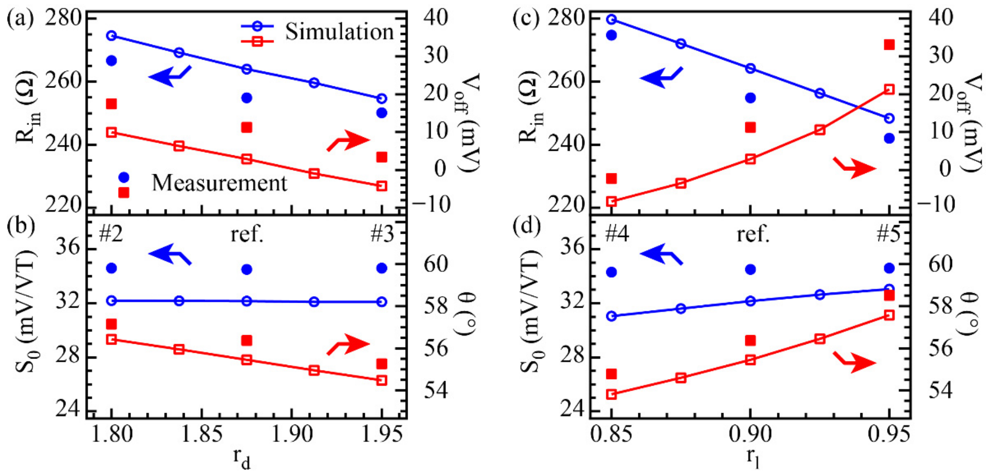

Figure 4: Measurement and simulation results for (a,b) a variable device diameter ratio r_d, and (c,d) a variable contact length ratio r_l (c) and (d). For both design parameters focus is on the input resistance R_{in} and single mode offset voltage V_{off} illustrated in the top graphs, and voltage related sensitivity magnitude S_0 and polar angle θ shown in the bottom graphs.

Table 2. Figures of merit for the different design variants.

Device	R_{in} (Ω)	V_{off} (mV)	S_0 (mV/VT)	θ (°)
Ref. device	255	11	34.5	56.4
#2	267	18	34.6	57.2
#3	250	3	34.6	55.3
#4	275	−2	34.3	54.8
#5	242	33	34.6	58.5

investigated parameter range. Further there is an optimum value of r_l of about 0.86 resulting in a device with zero offset voltage. S_0 and θ_{av}, shown in Fig. 4(d), increase with increasing r_l. The device #4 with $r_d = 1.875$, $r_a = 0.0.85$ and $r_w = 0.019$ achieves a polar angle of $\theta = 54.8°$ with an offset of $V_{off,av} = -2°$mV and is therefore close to a device with an isotropic response and zero offset. The magnitude of the three sensitivity vectors, i.e., $S_1 = 34.3$ mV/V, $S_2 = 34.6$ mV/V, $S_3 = 34.1$ mV/V, are closely matched and comparable to conventional Hall plates.

4. Conclusion

A 3D Hall-effect sensor with an isotropic response and zero offset is feasible. In view of its symmetry, it can be operated with the same drive and compensation circuitry for its three sensitive directions. For further improvement of the sensitivity magnitude the contact width ratio r_w should be optimized. However the influence of such variation on the offset has to be clarified. Further it has to be noted that the present device is a discrete component lending itself for hybrid integration with drive and signal conditioning circuitry by multi-chip stacking assembly. Co-integration with on-chip circuitry will likely require additional technological developments, since the low doping of the silicon wafer used for the sensor is not standard for CMOS substrates.

References

[1] E. Ramsden, Hall Effect Sensors – Theory and Applications, 2nd ed., Elsevier, Netherlands, 2006.
[2] F. Burger, P-A. Besse, and R. S. Popovic, New fully integrated 3-D silicon Hall sensor for precise angularposition measurements, Sensors and Actuators A: Physical, vol. 67, pp. 72-76, 1998.
[3] O. Paul, R. Raz, T. Kaufmann, Analysis of the offset of semiconductor vertical Hall devices, Sensors and Actuators A: Physical, vol. 174, 2012, pp. 24-32.
[4] C. Sander, C. Leube, T. Aftab, P. Ruther, O. Paul, Isotropic 3D silicon Hall sensor, 28th IEEE International Conference on Micro Electro Mechanical Systems (MEMS), pp. 893-896, 2015.